Electron-Energy-Loss Spectroscopy and the Study of Solids

J. M. THOMAS,* B. G. WILLIAMS,* and T. G. SPARROW

Department of Physical Chemistry, University of Cambridge, Lensfield Road, Cambridge, CB2 1EP, U.K.

Received May 30, 1985 (Revised Manuscript Received August 27, 1985)

Electron-energy-loss spectroscopy (EELS) is a technique that yields chemical composition, oxidation states, bond distances, and, under favorable circumstances, the electronic structure of solids. It is a technique with obvious chemical significance especially since it can identify by simultaneous electron diffraction or real-space imaging the crystallographic phase under study. All this can be achieved by using conventional electron microscopes fitted with an appropriate electron spectrometer. Indeed the amount of material required for investigation is less than a picogram and can be of submicron dimensions.

Although EELS is not well-known, it is not a new technique.[1] Several decades ago it was used to detect the presence of carbon and other light elements by noting the discrete "loss" peaks suffered by primary beams of electrons as they penetrate thin films. Energy losses ascribable to K-shell ionization of ca. 285, 400, and 530 eV are found in films containing carbon, nitrogen, and oxygen. In recent years, largely as a result of seminal work by Propst and Piper[2] and others,[3] high-resolution electron-energy-loss spectroscopy (HREELS) has been used extensively for the study of adsorbed films at solid, especially metal, surfaces. With highly monochromatic primary beams of up to 20-eV energy, energy-loss peaks, resolvable to better than 20 meV, may be unambiguously assigned[4-7] to such linkages as W—H, Ni—D, CH_3—C≡, and linear and multiply bonded CO and hydrocarbon fragments in various states of hybridization. Likewise, on certain oxide films, notably alumina, inelastic loss tunnelling spectroscopy, pioneered by Jakelevic and Lambe[8] and adopted by others,[9,10] has also proved useful in pinpointing vibrational modes at solid surfaces.

It is not commonly appreciated that *low-resolution* electron-energy-loss spectroscopy, employing primary beams of up to 200 keV and an energy resolution of ca. 2 eV, can nowadays be readily accomplished[11-14] by using suitably adapted transmission electron microscopes (TEM). Figure 1 shows a schematic diagram of such a microscope. The various lenses serve to focus the incident electron beam onto the sample and the scattered electron beam onto the viewing screen. The apertures limit the angles and the divergences with which the various beams enter and leave the sample: the electron spectrometer is usually located below the phosphor screen. Increasingly, commercial, analytical electron microscopes are fitted with such spectrometers, although it is still more usual to have as an analytical attachment energy dispersive solid-state detectors that record the X-ray emission spectra. Scanning transmission electron microscopes (STEM), in which electron beams of ca. 0.3-nm diameter are used as probes, can enormously improve the spatial resolution attainable in electron-energy-loss spectroscopy. Owing to its rather better energy resolution it is also capable of yielding electronic band gaps and of probing the variation in electronic densities of states across interfaces. As STEM is significantly different from (and a much more expensive technique than) that based on TEM, we shall not, except parenthetically, dwell on the scope and advantages of EELS carried out with STEM. A useful review of the latter is given by Pennycook.[15]

Energy-Loss Processes: A Summary

A schematic diagram of the processes which one can observe in energy-loss microscopy and the associated energy-loss spectra are illustrated in Figure 2. The *zero-loss peak* is the result of electrons being scattered elastically in the forward direction. In low-resolution spectroscopy of the kind discussed here, this peak also includes the thermal diffuse scattering arising from the excitation of phonon modes in the sample. At relatively small energy losses (about 5–25 eV), *plasmon peaks* are observed. For the free electron metals, plasmons may be regarded as collective excitations of the whole sea of conduction electrons so that they yield information

Professor John M. Thomas (see *Accounts of Chemical Research*, **1985**, *18*, 118).

Dr. Brian G. Williams was born in South Africa and obtained his Ph.D. in the Cavendish Laboratory. Since 1968 he has been interested in Compton scattering and is editor of a definitive text on that subject. He has held visiting and lecturing posts in universities in Helsinki, Strathclyde, and Dar es Salaam. Presently he is a Senior Research Fellow of the Royal Society.

Timothy G. Sparrow is a Licentiate of the Institute of Physics. After 5 years working as a technician in industry (CIBA-Geigy, U.K., and Welding Institute, Cambridge), he became an assistant staff member in the Cavendish Laboratory in 1969 and joined the Department of Physical Chemistry in 1981. He has recently joined Cambridge Instruments.

(1) Rudberg, E. *Proc. R. Soc. London, Ser. A* **1930**, *127*, 111. Ruthemann, G. *Naturwissenschaften* **1941**, *29*, 648. Klemperer, O. "Electron Optics" Cambridge University Press: London, 1953. Pines, D. *Adv. Solid State Phys.* **1955**, *4*, 367. Klemerer, O.; Sheperd, J. P. G. *Adv. Phys.* **1963**, *12*, 355.

(2) Propst, F. M.; Piper, T. C. *J. Vac. Sci. Technol.* **1967**, *4*, 53.

(3) Froitzheim, H.; Ibach, H.; Lehwald, S. *Rev. Sci. Instrum.* **1975**, *46*, 1325. Ibach, H.; Mills, D. L. "Electron Energy Loss Spectroscopy and Surface Vibrations"; Academic Press: New York, 1982.

(4) Weinberg, W. H. *Annu. Rev. Phys. Chem.* **1978**, *29*, 115.

(5) Somorjai, G. A. "Chemistry in Two Dimensions"; Cornell University Press: Ithaca, NY, 1981.

(6) Rao, C. N. R.; Srinivasan, A.; Jagannathan, K. *Int. Rev. Phys. Chem.* **1981**, *1*, 45.

(7) Jayasooriya, M. A.; Chesters, M. A.; Howard, M. W.; Kettle, S. F. A.; Powell, D. B.; Sheppard, N. *J. Chem. Soc., Chem. Commun.* **1979**, 18.

(8) Jaklevic, R. C.; Lambe, J. *Phys. Rev. Lett.* **1966**, *17*, 1139.

(9) Hansma, P. K. *Phys. Rep.* **1977**, *30C*, 145.

(10) Skarlatos, Y.; Barker, R. C.; Haller, G. L.; Yelon, A. *J. Phys. Chem.* **1975**, *79*, 2587.

(11) (a) Isaacson, M. S.; Joy, D. C. In "EXAFS Spectroscopy"; Plenum Press: New York, 1981; pp 213, 269. (b) Leaman, R. D.; Grunes, L. A.; Fejes, P. L.; Silcox, J. *Ibid.* p. 217. (c) Thomas, J. M. *Ultramicroscopy* **1982**, *8*, 13. (d) Beer, M.; Carpenter, R. W.; Eyring, LeRoy; Lyman, C. L.; Thomas, J. M. *Chem. Eng. News.* **1981**, *59* (Aug 17), 40.

(12) Thomas, J. M. In "Inorganic Chemistry: Toward the 21st Century"; Chisholm, M. H., Ed., American Chemical Society: Washington, D.C., 1983, *ACS Symp Ser. No. 211*, 445.

(13) Colliex, C.; Krivanek, O. L.; Trebbia, P. In "Electron Microscopy and Analysis"; Inst. Phys. Conf. Series 61, 1982; pp 183–188.

(14) Egerton, R. F. In "Quantitative Electron Microscopy"; Chapman, J., Craven, A. J., Eds.; 25th Scottish Universities Summer School in Physics, 1984; pp 273–304.

(15) Pennycook, S. J. *Contemp. Phys.* **1982**, *23*, 371.

0001-4842/85/0118-0324$01.50/0

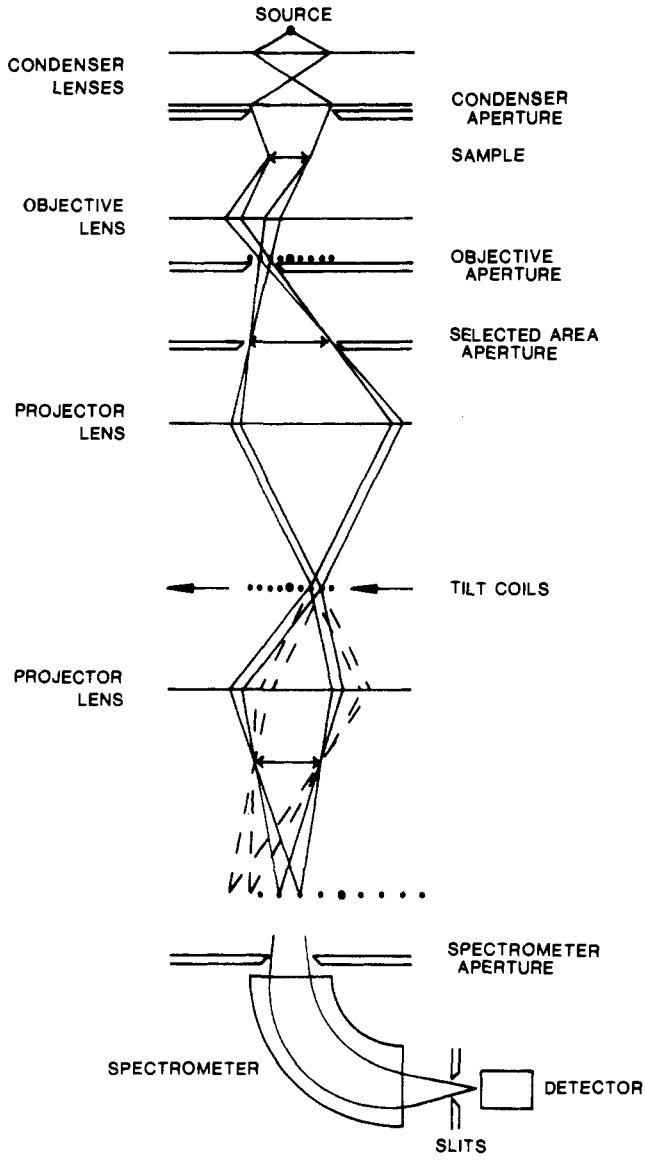

Figure 1. Schematic diagram of a transmission electron microscope fitted with an EELS spectrometer. Double headed arrows indicate image planes and rows of dots, diffraction planes.

relating to many-body effects in the electron gas. For insulators the analysis is more complicated and requires extensive band-structure calculations from which the energies and probabilities of the various interband transitions can be determined.[16]

Further along the energy-loss scale, steps occur at energies corresponding to those required to eject core electrons from the sample. When the energy loss is very high, however, the electron intensity becomes very low and the spectrum correspondingly lacks meaningful signal over noise. These considerations suggest 100–2000 eV as a preferred range of energy loss, which, in turn, means that the elements Li to Si (Z = 3 to Z = 14) can be detected via their K-shell losses, elements Si to Sr (Z = 14 to Z = 38) via their L-shell losses and elements Rb through Os (Z = 37 to Z = 76) via their M-shell losses, with a possibility of detecting even heavier elements by N-shell ionization. It is further worth noting that, whereas K and certain L edges are rather sharp, other L edges are somewhat rounded,

(16) Raether, H. "Excitation of Plasmons and Interband Transitions by Electrons" Springer Tracts in Modern Physics, Springer Verlag: Berlin 1980.

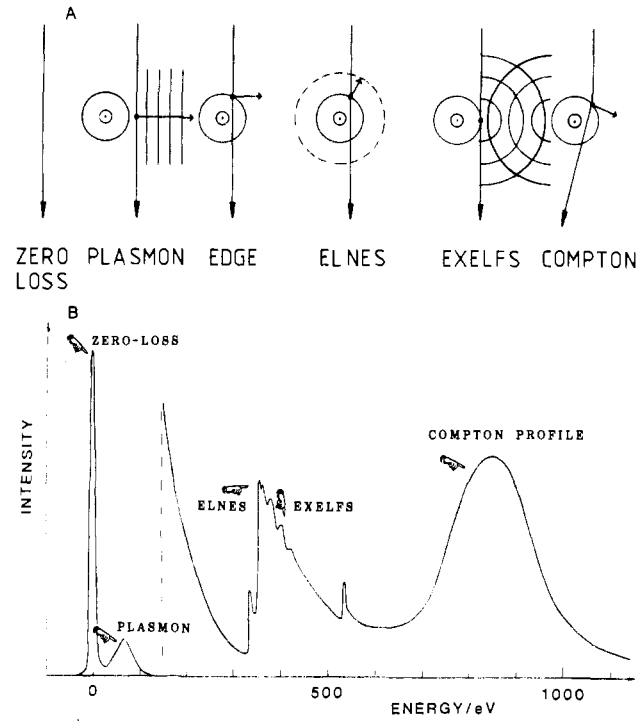

Figure 2. Schematic diagram of (A) the processes observed in EELS and (B) the corresponding spectrum. (The vertical dashed line in (B) indicates a change of scale.) ELNES stands for *electron-loss near-edge structure* and EXELFS for *extended energy-loss fine structure* (see text).

which renders their detection and measurement more difficult. It is prudent, therefore, to rely more on EDX (energy dispersive X-rays analysis)[11d] for the detection of medium and heavy elements. Because the cross sections for the excitation of the K- and L-shell electrons are known, the intensities of the electron-energy-loss edges can be used to determine the elemental composition of the sample.[14,17]

Closer examination of the edges shows that there is considerable structure commonly referred to as *energy-loss near-edge structure* (ELNES), the electron scattering counterpart of XANES or *X-ray absorption near-edge structure*. This depends on the density of unoccupied states near the Fermi energy as well as on the transition matrix elements, and therefore the symmetries of the initial and final states. The information retrievable from this region of the loss spectrum will, therefore, relate to the electronic structure, oxidation state, state of orbital hybridization, and site symmetry of the element under investigation.[18]

The ELNES structure extends typically up to about 20 eV beyond the edge but, with accurate data, one sees yet further structure extending an additional 200 or so volts. This *extended energy-loss fine structure* (EXELFS) arises when the ejected electrons are scattered by the neighboring atoms and interfere with themselves and is the electron scattering equivalent of EXAFS (*extended X-ray absorption fine structure*).[11a] It may, therefore, be used to obtain information about nearest-neighbor distances and coordination numbers. Later we shall compare the results of EXELFS mea-

(17) Leapman, R. D.; Rez, P.; Mayers, D. F. *J. Chem. Phys.* **1972**, *72*, 1232–1243.

(18) Leapman, R. D.; Grunes, L. A.; Fejes, P. L. *Phys. Rev. B: Condens. Matter* **1982**, *26*, 614–635. Grunes, L. A.; Leapman, R. D.; Wilker, C. N.; Hoffmann, R.; Kunz, A. B. *Phys. Rev. B: Condens. Matter* **1982**, *25*, 7157.

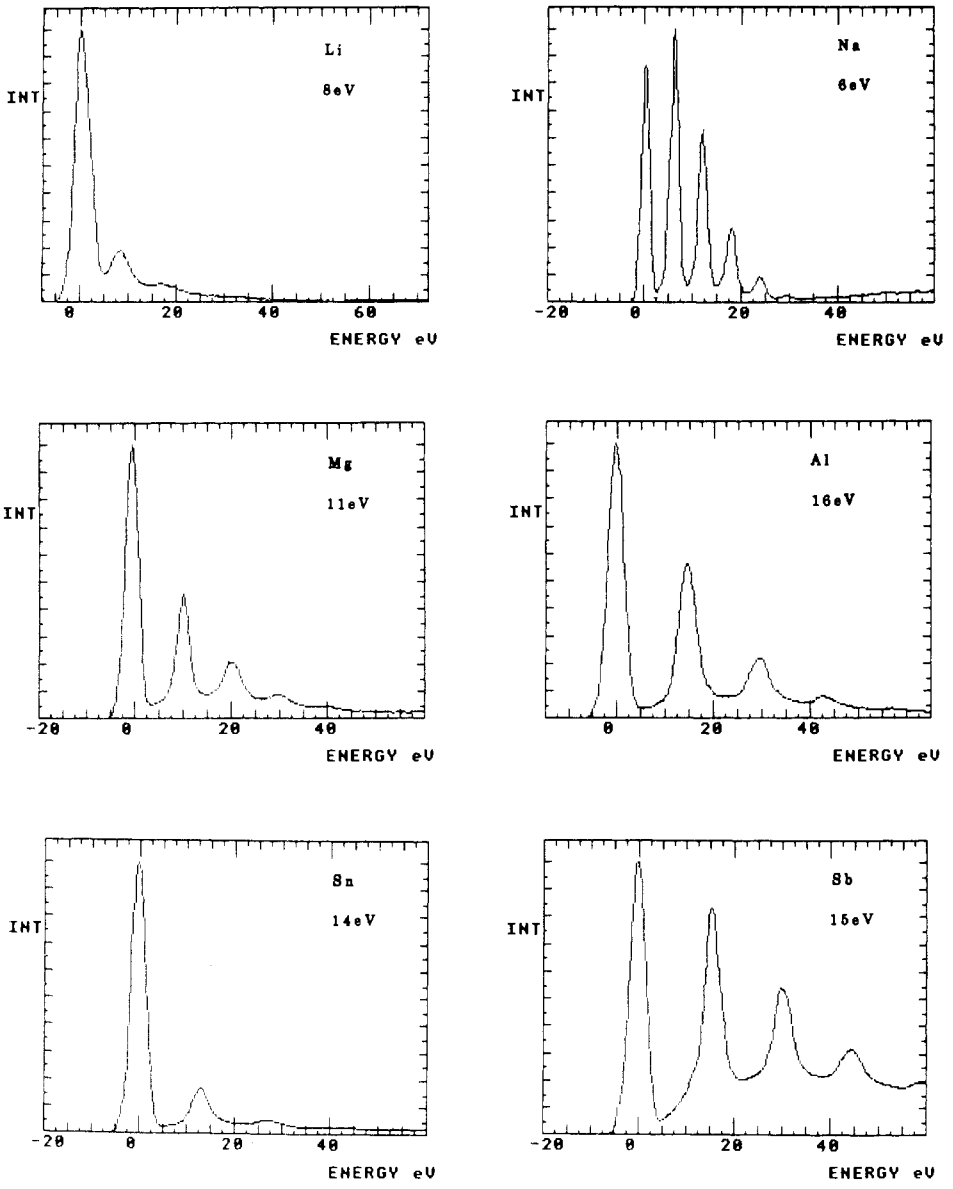

Figure 3. Measured plasmon spectra for various "free electron" materials.

surements on amorphous and crystalline alumina with those obtained from EXAFS.[19]

Finally, the electrons which have been scattered through an angle of about 5°, as distinct from those which pass straight through the sample, give rise to an entirely new feature: the electron scattering equivalent of the *Compton profile* which can be used to obtain a measure of the ground-state momentum wave function of the electrons in the sample.[20,21]

Plasmon-Loss Spectroscopy

Plasmon spectroscopy has, for many years, been the preserve of the physicists, particularly those concerned with many-body effects in the calculation of electronic structure.[16] For the free electron metals an expression for the plasma frequency may be obtained simply by imagining that the sea of electrons is displaced sideways and then released. The restoring force, arising from the separation of the positive and negative charges, is linear, the oscillation is harmonic, and the frequency of the bulk plasmon ω_p and therefore the plasmon energy E_p is given by

$$E_p = \hbar\omega_p = \hbar(ne^2/m\epsilon)^{1/2} \quad (1)$$

where n is the electron density and the other symbols have their usual meaning. This equation predicts the plasmon energies of free electron metals such as aluminium, sodium, magnesium, and so on, within a few percent and also works well for semiconductors such as silicon. For the alkali halides the predicted values are out by a factor of about 2. Under appropriate conditions one also observes surface plasmons the energy of which is $1/(2)^{1/2}$ times that of the bulk plasmon when the metal surface is exposed to a vacuum.[16] Figure 3 shows a collection of plasmon spectra for various free electron metals. The successive peaks arise from the excitation of one or more plasmons, and the spacing between the peaks is given accurately by eq 1.

For the chemist, plasmon spectroscopy provides a convenient means for the qualitative identification of

(19) Bourdillon, A. J.; El Mashri, S. M.; Forty, A. J. *Philos. Mag. A* **1984**, *49*, 341–352.
(20) Williams, B. G.; Thomas, J. M. *Int. Rev. Phys. Chem.* **1983**, *3*, 39–82. Williams, B. G.; Parkinson, G. M.; Eckhardt, C. J.; Thomas, J. M.; Sparrow, T. G. *Chem. Phys. Lett.* **1981**, *78*, 434.
(21) Williams, B. G.; Sparrow, T. G.; Egerton, R. F. *Proc. R. Soc. London, Ser. A* **1984**, *393*, 409–422.

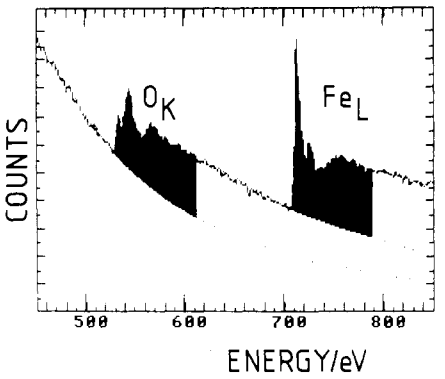

Figure 4. EELS spectrum of Fe_2O_3 showing the oxygen K edge at 532 eV and the iron L edge at 708 eV. The dotted lines are the fitted backgrounds, and the darkened regions indicate the areas used for quantitative chemical analysis.

materials if one is able to recognize the plasmon "fingerprint".[22] The utility of plasmon spectroscopy is made clearer if one notes that the energy-loss spectrum is usually dominated by the plasmon losses. Furthermore, because the intensity in the various plasmon lines follows a Poisson distribution, it follows that the sample thickness is proportional to the logarithm of the ratio of the total intensity in the plasmon lines to the intensity in the zero-loss peak.[21] To obtain absolute, rather than relative, thicknesses a calibration is needed which requires either the calculation of the plasmon cross section or an independent measurement on a sample of known thickness. Using plasmon spectra in this way it is possible to determine the thickness of films up to several thousand nanometers with a precision of a few percent.[23]

Plasmon loss spectra, apart from yielding good estimates of the thicknesses of thin films, are also valuable for identifying the products of decomposition (either electron-beam-induced or stimulated by heat or light) of mixed hydrides (e.g., $LiAlH_4$ or $NaBH_4$) and in pinpointing compositional variations as between metal, hydride, and oxide in preparations of main group hydrides and their solvates.[22,24]

Chemical Analysis

Further out in the energy-loss spectrum is the edge at an energy transfer corresponding to the binding energy of the core electrons in the sample,[25] and this is illustrated for Fe_2O_3 in Figure 4. The oxygen K edge at 532 eV as well as the iron edge at 708 eV is clearly evident. If an appropriate background is subtracted, the intensity under the edge can be measured over a suitable energy range, and from the calculated cross sections for exciting each edge, the amount of each element which is present can be determined.[12,14] Apart from the fact that it is an "absolute"technique requiring no standard for calibration, the special advantage possessed by EELS as a means of chemical analysis is that it combines sensitivity with spatial resolution. It is, in a literal sense, an ultramicro method with minimum detectable amounts, in favorable circumstances, of better than 10^{-20} g. Its especial advantage in being able to cope with the light elements makes it a very useful tool for certain applications. Thus, EELS was successfully used by Leapman et al.[26] to identify the composition of needle-shaped precipitates in Cr–Mo steel as Cr_2N and that of granular precipitates as $Fe_5C_{18}C_6$. In studying Si–Al–O–N ceramics, EELS has been particularly useful in determining local composition at both crystalline and contiguous amorphous regions. And in the study of graphite intercalates and graphite fluorides[27] EELS has yielded local compositional information, again illustrating its superiority in coping with the analysis of the light elements. Two remarkable recent triumphs of electron energy loss as an analytical tool are (i) the detection of nitogen[28] in the minute platelets,[30] lying on {100} planes, in type 1a diamonds, and (ii) the establishment of the stoichiometry of thin films of semiinsulating polysilicon (such as those used in the technology of integrated circuits) as $Si_{0.50\pm0.05}O$, a value in good agreement with the results of Rutherford back-scattering.[29] In the study of biomineralization its potential utility needs no further elaboration.

Electron-Loss Near-Edge Structure (ELNES)

By fitting an appropriate background to the region immediately before the edge and then subtracting it from the main spectral feature, the structure associated with the edge stands out clearly. To explain the ELNES in detail requires extensive calculations[18] of the energy density of states, the effect of the core hole which remains when an electron is excited as well as the transition matrix elements. Fairly simple arguments do, however, give us some insight into the reasons for the observed structure and may serve to guide us in formulating the problems which we might hope to address using ELNES.

In Figure 4 it is seen that two sharp lines are present at the metal L edge. The transition-metal d bands are relatively narrow, having a width of only a few electronvolts, so that all transitions from core levels to the d band will have more or less the same energy and sharp lines are observed at their L edges. In addition, the L level is split with the $2p_{1/2}$ and $2p_{3/2}$ levels having different energies so that there are two lines at the edge and the separation of the lines is given accurately by the known splitting between these two levels taken from atomic spectra. Finally, the effect of the selection rules is seen in the fact that the L_1 line is absent since the allowed transitions must satisfy the spin selection rule $\Delta l = \pm 1$.

The transition probability in the excitation process will be proportional to the energy density of final states so that, if electrons are removed from the d band, the intensity of these lines should increase relative to the intensity in the shoulder, which arises from transitions to the continuum, and these intensities can be used to

(22) Sparrow, T. G.; Williams, B. G.; Thomas, J. M.; Jones, W.; Herley, P. J.; Jefferson, D. A. *J. Chem. Soc., Chem. Commun.* **1983**, 1432–1435.
(23) Ferrell, R. A. *Phys. Rev.* **1956**, *101*, 554.
(24) Jones, W.; Sparrow, T. G.; Williams, B. G.; Herley, P. J. *Mater. Lett.* **1984**, *2*, 377–379.
(25) Rao, C. N. R.; Sparrow, T. G.; Williams, B. G.; Thomas, J. M. *J. Chem. Soc., Chem. Commun.* **1984**, 1238–1240.
(26) Leapman, R. D.; Sanderson, S. J.; Whelan, W. J. *Met. Sci.* **1978**, 215.
(27) Egerton, R. F. In "37th Annual Proceedings of Electron Microscopy Society of America"; Bailey, G. W., Ed., Claitors: Baton Rouge, 1979; p 128.
(28) Berger, S. D.; Pennycook, S. J. *Nature (London)* **1982**, *298*, 635. Bursill, L. A.; Egerton, R. F.; Thomas, J. M.; Pennycook, S. J. *J. Chem. Soc., Faraday Trans. 2* **1981**, *77*, 1367.
(29) Wong, J.; Thomas, J. M.; Jefferson, D. A.; Sparrow, T. G.; Milne, R.; Howie, A.; Koch, E. E., in preparation.
(30) Evans, T.; Phaal, C. *Proc. R. Soc. London, Ser. A* **1962**, *270*, 535.

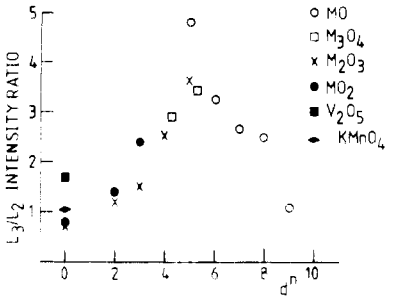

Figure 5. Measured L_3/L_2 ratios for 3d transition-metal oxides plotted against the number of d electrons. The samples used were V_2O_5, V_2O_3, CrO_2, Cr_2O_3, MnO, Mn_3O_4, Mn_2O_3, MnO_2, $KMnO_4$, FeO, Fe_3O_4, Fe_2O_3, and CuO.

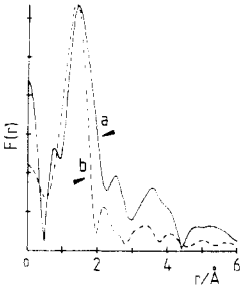

Figure 6. Fourier transformed EXELFS data for α-alumina (solid line) and amorphous alumina (dashed line) before correcting for the phase shift. The Al–O distance for amorphous alumina is 1.89 Å.[19]

determine the number of d electrons in transition-metal compounds. Furthermore, since the degeneracy of the L_3 level is 4 while that of the L_2 level is 2 one might expect the ratio of the intensities in these two lines to be 2. However, it is found that this ratio departs quite significantlyfrom 2.[31] This is illustrated in Figure 5, where the number of d electrons in a series of 3d transition-metal oxides is plotted against the L_3/L_2 intensity ratio[32] and this ratio increases as the number of d electrons increases from 0 to 5 and then decreases as the d band is filled further. It is apparent, therefore, that the L_3/L_2 ratio provides another probe of the oxidation state of the metal. In this connection it is relevant to quote the elegant work of Brown et al.[33] on the EELS fine structure of rare-earth sesquioxides. The number of 4f electrons present in the rare-earth ions (from La to Lu) correlates smoothly with both the M_5–M_4 energy separation and the M_5/M_4 intensity ratio. The analytical utility of facts such as these is obvious although the theoretical reasons for the latter correlations remain unclear.

An important extension of this work is to site-specific studies in which the EELS spectra are used to obtain information about the positions of selected atoms within the unit cell. It is well-known[34] that by choosing the orientation of the incident beam with respect to the orientation of the crystal a standing-wave field can be set up in the crystal in such a way that the beam current is a maximum at the lattice planes or alternatively so that it is a maximum midway between the lattice planes. Depending on the position of a particular atom within the unit cell, the contribution from the relevent feature in the EELS spectrum will be either enhanced or diminished. Tafto and Krivanek[35] have studied a chromite spinel in this way and from the variation in the strengths of the oxygen K edge and the chromium and iron L edges they confirmed the positions of the cations in the unit cell and were able to determine the location of the Fe^{2+} and Fe^{3+} ions within the cell.

Extended Electron-Loss Fine Structure (EXELFS)

Beyond the near-edge structure, extending over several hundred electronvolts, is the extended electron energy-loss fine structure. EXELFS is not easy to record accurately[36] which explains in part why the full scope of EXELFS measurements has not yet been realized. As the ejected electron tries to escape from its parent atom, it is scattered by the neighboring atoms. Depending on the wavelength of the electron and the distance to the nearest-neighbor atoms, the reflected wave will interfere destructively or constructively with that of the ejected electron. If this interference is destructive, the probability of such an event occurring will be diminished, and if it is constructive, it will be enhanced. The effect will be weak but we expect the probability of any energy loss occurring to be modulated sinusoidally by a term of the form

$$\chi = N \exp(2\pi i 2R/\lambda) \qquad (2)$$

where λ is the wavelength of the ejected electron, R is the nearest-neighbor distance, and N is the number of atoms in the first coordination shell. The factor of 2 is to allow for the fact that the electron must go to the nearest neighbor and back. Since $2R$ must be about 4 or 5 Å, the electron energy must be about 50 eV or more, so that the EXELFS will occur in the region extending a few hundred volts beyond the edge.

The actual situation is rather more complicated than that outlined above, and a number of terms must be added to eq 2 to account for the phase change on reflection, the decay of the electron wave as it spreads out from the parent atom, irregularities in the arrangements of the atoms either because of thermal vibrations or because the sample is amorphous, and so on. However, these effects are reasonably well understood[36] and the important point is that the energy-loss spectrum shows oscillations beyond the near edge structure, the wavelengths of which depend on the distances between the atoms and the amplitudes of which depend on the number of atoms in each coordination shell.

EXELFS experiments on crystalline and amorphous alumina have recently been reported by Bourdillon, El Mashri, and Forty,[19] following important early work by Leapman and Cosslett.[37] Bourdillon et al. studied the oxygen edge which occurs at 532 eV, the samples in each case being about 300 Å thick. It is important to use such thin films since the quality of EXELFS spectra is corrupted by multiple scattering if the samples are too thick. A low order polynomial was fitted on a log-

(31) Leapman, R. D.; Grunes, L. A. *Phys. Rev. Lett.* **1980**, *45*, 397–401.
(32) Thomas, J. M.; Rao, C. N. R.; Williams, B. G.; Sparrow, T. G. *J. Phys. Chem.* **1984**, *88*, 5770–5772.
(33) Brown, L. M.; Colliex, C.; Gasgnier, M. *J. Phys., Colloq. C2, Suppl. No 2* **1984**, *45*, 433.
(34) Hirsch, P. B.; Howie, A.; Nicholson, R. B.; Pashley, D. W.; Whelan, M. J. "Electron Microscopy of Thin Crystals"; Krieger: New York, 1977.
(35) Tafto, J.; Krivanek, O. L. *Phys. Rev. Lett.* **1982**, *48*, 560–563.
(36) Leapman, R. D.; Grunes, L. A.; Fejes, P. L.; Silcox, J. In "EXAFS Spectroscopy: Techniques and Applications"; Teo, B. K., Joy, D. C., Eds., Plenum Press, New York, 1981.
(37) Leapman, R. D.; Cosslett, V. E. *J. Phys. D.* **1976**, *9*, 129.

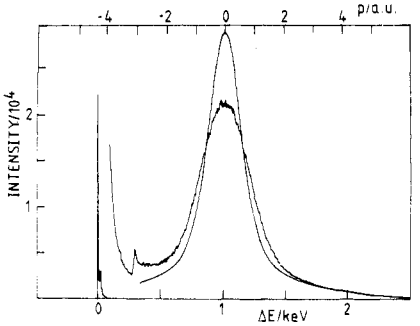

Figure 7. Compton profile of amorphous carbon measured by using an electron microscope. The solid line gives the Compton profile for a free atom of carbon for comparison. The plasmon line occurs close to the zero-loss peak, and the K edge at 284 eV is evident.

arithmic plot over the region above the edge, and this was then subtracted from the observed data. Fourier transformation then yielded the amplitudes and the phases of the oscillations, and the result of this is shown in Figure 6. From the known mean bond length in α-alumina they obtained a value for the phase change equivalent to a shift of 0.49 Å which is close to the calculated value of 0.51 Å. They were then able to determine the bond length in amorphous alumina and obtained a value of 1.89 Å in good agreement with EXAFS data which gave 1.90 Å.

Although it is difficult to obtain EXELFS data of the quality which one now expects to get almost routinely using EXAFS, the great promise (to some extent realized) of EXELFS lies in the fact that one can study truly microscopic regions as well as edges from light elements which are not readily accessible for studying by EXAFS. Light elements are amenable to studies using synchrotron radiation if total secondary electron yields are used as a measure of absorption: in this way one records SEXAFS rather than EXAFS. Also, with use of laser plasma produced Brehmstrahlung radiation as the primary source,[38] it is feasible to record EXAFS spectra for elements with atomic number up to about 20.

Compton Scattering

If, instead of measuring the energy-loss spectrum of the electrons scattered in the forward direction, we record the "loss" spectrum of the electrons which have been scattered through an angle of about 5° an entirely new feature is evident (Figure 7). This is the Compton profile.[20,21] When both the energy and the momentum transfer are large an electron in the sample is ejected from its ground state into a plane-wave final state.[39] The equations for the conservation of energy and momentum may then be solved to obtain an expression for the energy transferred in the scattering process. For stationary electrons the energy transfer depends only on the scattering angle and increases as the scattering angle increases. Because the electrons in the sample are moving, there will be an additional Doppler broadening of the energy distribution of the scattered radiation: both the peak shift and the Doppler broadening can be seen in Figure 7. As is always the case with the Doppler effect, the broadening depends on only one

(38) Key, M. H. *Plasma Physics Controlled Fusion* **1984**, *26*, 1383.
(39) Bonham, R.; Wellenstein, H. F. In "Compton Scattering"; Williams, B. G., Ed.; McGraw-Hill: New York, 1977.

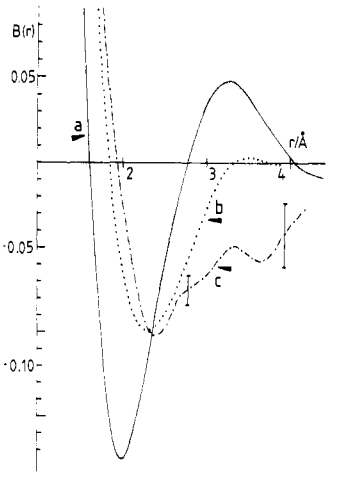

Figure 8. Reciprocal form factors for (a) diamond, (b) graphite, and (c) amorphous carbon. The amorphous material showed essentially no rings in the electron diffraction pattern. By probing the momentum of the valence electrons using electron beams, we infer from the closeness of curves (b) and (c)[40] that the local bonding is more graphitic than adamantine.

component of the momentum and this direction is defined by the scattering vector.

To relate experimental Compton profiles to theoretical models, we require the momentum wave function $\chi(p)$ which is the Fourier transform of the position wave function $\psi(r)$

$$\chi(p) = h^{-3/2} \int\int\int_{-\infty}^{+\infty} e^{-ipr/h}\psi(r)\, dr \qquad (3)$$

The momentum density $\rho(p)$ is the square modulus of the momentum wave function just as the position or charge density is the Fourier transform of the position wave function so that

$$\rho(p) = \chi^*(p)\chi(p) \qquad (4)$$

and finally, to obtain the Compton profile the momentum density must be averaged over planes in space so that

$$J(p_z) = \int\int_{-\infty}^{+\infty} \rho(p)\, dp_x dp_y \qquad (5)$$

With the aid of these equations the Compton profile may be used to probe the ground-state wave function of the electrons in the sample.

To illustrate the sensitivity of the Compton profile to changes in the wave function, the solid line (Figure 7) is a theoretical Compton profile for a free atom of carbon so that the differences between this and the experimental data show the magnitude of the changes which take place when bonds are formed from the free atom wave functions.

Since it is easier to think intuitively in position space than in momentum space, the analysis of Compton profile data is greatly facilitated if one Fourier transforms the profile in order to revert back to position space. Now, the Fourier transform of the charge density is the form factor so the Fourier transform of the momentum density has been called the reciprocal form factor (RFF). And since the Fourier transform of a product is the convolution of the Fourier transforms, the RFF is the convolution of the position space wave function with itself. More precisely, if $B(z)$ is the Fourier transform of $J(p_z)$, the Compton profile mea-

sured with the scattering vector in the p_z direction, then

$$B(\mathbf{r}) = \psi(\mathbf{r})^*\psi(\mathbf{r}) \quad (6)$$

where the asterisk indicates convolution.

Figure 8 shows the Fourier transformed Compton profiles of amorphous carbon, graphite, and diamond.[40] In all three cases there is a significant negative dip at a distance of about 2 Å. Now the RFF is a self-convolution so the negative dip reflects changes in the sign of the wave function and therefore the relative contributions of the s and p orbitals to each of the bonds. Indeed, the position of the dip depends primarily on the bond length and the size of the dip reflects the hybridization state.[41] In this particular example, Compton scattering shows clearly that the bonding in amorphous carbon is predominantly graphitic rather than adamantine. To analyze the electronic structure of the bonds in more detail requires rather extensive modelling of the wave function but this example illustrates the sensitivity of Compton scattering. Similar measurements on amorphous silicon should yield information about the bonding but it is important to avoid contamination with carbon which appears to be a rather more serious problem than is generally recognized.

Concluding Remarks

The experiments described in this Account, involving the study of solids by low-resolution EELS, have been carried out by using an electron microscope which, although updated, is of ancient vintage. Consequently the electron beams used as probes have a diameter never less than about 2 to 3 × 10^2 nm. In modern electron microscopes it is possible to reduce the beam diameter to less than 5 nm (and with STEM instruments, mentioned above, to less than 0.3 nm). The fact that, by reducing the beam diameter alone, one may improve the spatial discrimination and subsequent sensitivity by some 4 orders of magnitude is clearly a great advantage. Equally, with the advent of even more sensitive detection systems spectra of higher resolution may be registered by employing instruments such as those already operational in Zeitler's group.[42] The best commercial STEM instruments possess an energy resolution of ca. 0.7 eV which offers attractive scope in the study of ELNES and EXELFS.[43] One can forsee that with electron microscopes operating under vacua of 10^{-10} torr or better, surface chemical studies (such as the change in the frequencies of the surface plasmons broght about by adsorption[44]) may be routinely feasible.

It must be recognized that, although EELS is a powerful technique for characterizing solids, it is not likely to become universally applicable because there are many solids that are intrinsically susceptible to damage under electron irradiation.[45-48] Most, but by no means all, inorganic solids are rather beam resistant; broadly speaking organic materials, with some notable exceptions (e.g., those based on certain porphyrins), are beam sensitive and tend to yield poor EELS spectra. Nevertheless, as chemists focus more on the problems of microlithography, derivitization of surfaces, and the use of naked metal and bimetallic clusters, EELS is likely to play an increasingly prominent role as an investigative tool.

We acknowledge with gratitude support from the science and Engineering Research Council, the Royal Society, and the University of Cambridge. We also thank Dr. D. A. Jefferson for his role in converting a 40-year-old electron microscope into a versatile electron-energy-loss spectrometer.

(40) Williams, B. G.; Sparrow, T. G.; Thomas, J. M. *J. Chem. Soc., Chem. Commun.* **1983**, 1434.
(41) Williams, B. G.; Vasudevan, S.; Rayment, T. *Proc. R. Soc. London, Ser. A* **1983**, *388*, 219–228.
(42) Zeitler, E. private communication to J. M. Thomas, 1985.
(43) Batson, P. E.; Treacy, M. M. J. In "Proceedings of the 38th Electron Microscopy Society of America Meeting", San Francisco, 1980; Bailey, G. W., Ed.; Claitors: Baton Rouge, 1980; p 126.
(44) Küppers, J. *Surf. Sci.* **1973**, *36*, 53.
(45) Jones, W. In "Surface and Defect Properties of Solids"; Roberts, M. W., Thomas, J. M., Eds.; The Chemical Society: London, 1976; Vol. 5, p 5.
(46) Thomas, L. E.; Humphries, C. J.; Duff, W. R.; Grubb, D. T. *Radiat. Eff.* **1970**, *3*, 89.
(47) Parkinson, G. M.; Jones, W.; Thomas, J. M. In "Electron Microscopy at Molecular Dimensions: State of the Art and Strategies for the Future"; Baumeister, W., Vogell, W., Eds.; Springer-Verlag: Berlin, 1980; p 208.
(48) Downing, K. H.; Glaeser, R. M. "Proceedings of the 40th Annual Meeting of the Electron Microscopy Society of America".; Bailey, G. W. Ed.; Claitors: Baton Rouge, 1982.